

Lawrence Berkeley National Laboratory

Recent Work

Title

Linking Thermal, Hydrological and Mechanical Processes in Fractured Rocks

Permalink

<https://escholarship.org/uc/item/8zw2t6kc>

Journal

Annual Review of Earth and Planetary Sciences, 27

Author

Tsang, Chin-Fu

Publication Date

1998-07-01



ERNEST ORLANDO LAWRENCE BERKELEY NATIONAL LABORATORY

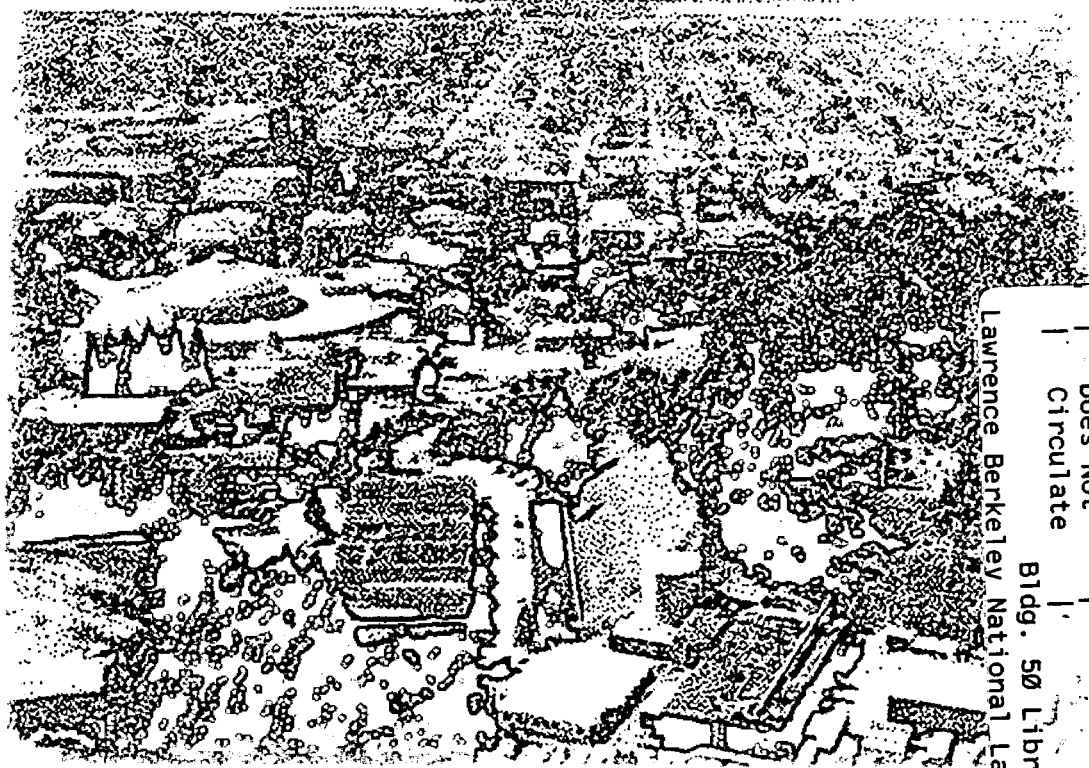
Linking Thermal, Hydrological and Mechanical Processes in Fractured Rocks

Chin-Fu Tsang

Earth Sciences Division

July 1998

Submitted to
Annual Review
of Earth and
Planetary Sciences



REFERENCE COPY |
Does Not |
Circulate |
Lawrence Berkeley National Laboratory
Bldg. 50 Library - Ref.
Copy 1
LBLN-42085

DISCLAIMER

This document was prepared as an account of work sponsored by the United States Government. While this document is believed to contain correct information, neither the United States Government nor any agency thereof, nor the Regents of the University of California, nor any of their employees, makes any warranty, express or implied, or assumes any legal responsibility for the accuracy, completeness, or usefulness of any information, apparatus, product, or process disclosed, or represents that its use would not infringe privately owned rights. Reference herein to any specific commercial product, process, or service by its trade name, trademark, manufacturer, or otherwise, does not necessarily constitute or imply its endorsement, recommendation, or favoring by the United States Government or any agency thereof, or the Regents of the University of California. The views and opinions of authors expressed herein do not necessarily state or reflect those of the United States Government or any agency thereof or the Regents of the University of California.

Linking Thermal, Hydrological and Mechanical Processes in Fractured Rocks

Chin-Fu Tsang

Earth Sciences Division
Ernest Orlando Lawrence Berkeley National Laboratory
University of California
Berkeley, California 94720

July 1998

The paper is prepared with joint funding from the Swedish Nuclear Power Inspectorate (SKI), Stockholm, Sweden, and the Office of Energy Research, Office of Basic Energy Sciences, Engineering and Geosciences Division, of the U.S. Department of Energy under Contract No. DE-AC03-76SF00098. This research used resources of the National Energy Research Scientific Computing Center, which is also supported by the Office of Energy Research of the U.S. Department of Energy.

CONTENTS

Abstract	1
Background.....	2
Mathematical Formulation of Coupled Processes Linking THM Effects.....	3
Two Examples of Coupled Processes.....	6
Three Current THM Field Experiments	8
<i>Kamaishi Coupled THM Experiment</i>	9
<i>The FEBEX Experiment</i>	11
<i>The Drift Scale Heater Test</i>	14
Summary and Concluding Remarks.....	16
<i>Acknowledgements</i>	16
<i>Literature Cited</i>	17

Linking Thermal, Hydrological and Mechanical Processes in Fractured Rocks

Chin-Fu Tsang

Earth Sciences Division
Ernest Orlando Lawrence Berkeley National Laboratory
University of California
Berkeley, California 94720

ABSTRACT

In this paper, an overview is presented of coupled processes linking thermo-hydro-mechanical (THM) effects in fractured rocks. A formulation is first presented to show the linkage mathematically, which can be used as a basis for numerical solutions and for further developments. Two simple examples of hydromechanical (HM) and thermo-hydro-mechanical (THM) coupled processes are discussed to convey physical insight into such couplings. Finally, three large-scale, long-term experiments currently under way are described. These are being conducted specifically to study coupled processes in situ.

BACKGROUND

Over the last ten years or so, there has been intensive research on the processes that link thermal gradients, hydrologic flow and mechanical deformation in fractured rock. Much of this work was summarized and discussed in a number of review papers and edited books (Tsang, 1987, 1991; IJRMMS, 1995; Stephansson et al., 1996; Haijink, 1995). The main impetus for this intense activity has been the need to evaluate the impacts of these linked or coupled processes on the safety or isolation potential of a nuclear waste repository.

A nuclear waste repository is essentially an excavated underground cavity composed of tunnels and openings in which radioactive waste is emplaced. This waste releases heat, which causes expansion in the rock, closing of rock fractures, and disturbances of fluid flow in adjacent rock formations. Often, canisters containing the waste are surrounded by buffer or backfill materials after being placed in the repository. The coupling of thermal (T), hydro (H) and mechanical (M) effects also occurs in these materials. In order to give more definite examples of these coupled processes and point out relevant issues, we shall divide the repository problem into two stages: the construction stage, when no heat-releasing waste has yet been emplaced and only coupled HM processes in rock are expected; and the operation and containment stage, when waste, buffer and backfill materials are present and coupled thermal-hydro-mechanical (THM) processes will occur.

During the first stage, the excavation of the repository causes a major perturbation of the rock mass. The impact depends on the initial stress field around the system, the nature of the excavation method and the repository design. It is not easy to determine the in situ stress field of a region, especially in the presence of fracture sets forming a network, which could well be anisotropic and may not even follow a regular ellipsoidal angular distribution. The excavation will cause stress concentration around the opening, which in turn changes the local fracture apertures and permeability. The change in the aperture and permeability of a fracture is a function of normal and shear stresses across it. An increase in normal stress will cause the fracture aperture to close and the permeability will decrease as the square of the aperture. However, the aperture decrease will stop at an "irreducible" aperture after the normal stress reaches a certain high value. The fracture permeability change with changes in shear stress is more complex, involving possible effects of gouging, asperity deformation, etc. In these cases the permeability can easily change by one order of magnitude. In general, the question is how to determine the anisotropic change in hydraulic conductivity around the repository cavity. The excavation also represents a relatively sudden event, and hence the normal and shear stress across nearby fractures may change in a short time, producing sudden aperture changes. This sudden change in stress may cause the pore pressure to rise quickly, before the water has had a chance to move and equilibrate. Such a transient coupled HM effect may cause local failures and create microfractures, as well as local hydraulic conductivity changes.

During the operation and isolation stage of a nuclear waste repository there is thermal input, and a series of THM processes will occur. The heat from the nuclear waste will cause a rise in the temperature of the buffer/backfill and the rock, as the repository is being filled. The temperature will peak after a time period estimated to be a few hundred years. Thermally induced stresses are found around the repository, which may change the hydraulic conductivity, as discussed above. The TM effects have been relatively well studied and much experience has been gained in its

modeling and observation. However, what is interesting here is the progressive heating of the multiple media system, i.e., the waste canister, backfill materials, which could be bentonite, and then the surrounding rock, each of which has a different expansion coefficient. How they deform relative to each other and how the interfaces between them behave may make a difference in the hydraulic properties of these interfaces. In the worst-case scenario, these interfaces may form relatively higher hydraulic-conductivity paths for water flow. The heat will also induce convective flow in rock. Convective flow depends on thermal energy imparted to the fluid and would last much longer than the temperature peak time. In the very near field where the local temperature may be high, vaporization will occur. The vaporized water will move away from the repository and condense in cooler regions of the rock. All this forms a complex and dynamic hydrologic system that requires a fully multiphase code for its analysis. How the thermohydraulic process will affect the effective stress and thus the mechanical condition of the fracture-porous rock is an open question.

MATHEMATICAL FORMULATION OF COUPLED PROCESSES LINKING THM EFFECTS

A number of authors have presented alternative formulations of coupled processes linking THM effects. Many of these approaches are summarized in Jing et al. (1995). In this section we shall present, without development, the governing equations originating from the work of Noorishad and Tsang (1996), which can be consulted for details. The goal is to describe how the linkage of THM effects can be represented mathematically.

For saturated rock (i.e., rock saturated with water without the presence of air), the mathematical equations linking THM effects may be expressed in three governing and two constitutive equations. The first describes the combined mass and momentum balance law for moving fluid:

$$\frac{\rho_\ell}{\rho_o} \frac{\partial e}{\partial t} + \phi \beta_P \frac{\partial p}{\partial t} + \phi \beta_T \frac{\partial T}{\partial t} = \nabla \left[\frac{\rho_\ell k_\ell}{\rho_o \eta_\ell} (\nabla P + \rho_\ell g \nabla z) \right] \quad (1)$$

where ρ_ℓ is density of fluid in the rock
 ρ_o is density of reference fluid
 η_ℓ is liquid dynamic viscosity
 k_ℓ is the local intrinsic permeability tensor
 ϕ is the rock porosity
 β_p is compressibility coefficient of the liquid
 β_T is the thermal volume expansion coefficient
 g is the gravity constant
 P is the liquid pressure
 T is the temperature
 e is the rock matrix volume strain
 z is the elevation

The terms on the left-hand side of Equation (1) describe the changes in rock volume due to strain, pressure and temperature, respectively. The right-hand side gives the liquid flow due to pressure

gradient and gravity according to Darcy's Law. The second governing equation is the mechanical equation of motion:

$$\frac{\partial \tau_{ij}}{\partial x_j} + \bar{\rho}_s f_i = \rho \frac{\partial^2 U_i}{\partial t^2} \quad (2)$$

where τ_{ij} is the stress tensor
 f_i is the body force
 $\bar{\rho}_s$ is the average specific mass of the rock
 U_i is the displacement
 ρ is the density of the liquid-filled rock

The third governing equation describes the conservation of energy:

$$(\rho C)_m \frac{\partial T}{\partial t} + T_o \gamma \frac{\partial}{\partial t} (\delta_{ij} e_{ij}) + \rho_\ell C_{v\ell} \frac{k_\ell}{\eta_\ell} (\nabla P - \rho_\ell g \nabla z) \nabla T = \nabla K_m \cdot \nabla T \quad (3)$$

where $(\rho C)_m$ is the specific heat capacity of the liquid-filled medium
 K_m is the thermal conductivity of the liquid-filled medium
 T_o is the absolute temperature in the stress-free state
 δ_{ij} is 1 for $i = j$ and 0 for $i \neq j$
 e_{ij} is strain components of the rock
 $C_{v\ell}$ is the liquid specific heat constant at constant volume
 $\gamma = (2\mu + 3\lambda)\beta$ with β being the isotropic linear solid thermal expansion coefficient and μ and λ being Lamé's constants

The first term on the left-hand side of Equation (3) is the change in energy; the second term describes the deformation conversion energy; and the third term represents the convective energy due to heat carried by the moving liquid. The right-hand side gives the temperature conduction in the liquid-filled rock medium.

The following two constitutive equations complete the mathematical description of the coupled processes linking T, H, and M:

$$\zeta = \frac{\rho_\ell}{\rho_o} \times \delta_{ij} e_{ij} - \frac{1}{M} P + \frac{1}{M_T} T \quad (4)$$

$$\tau_{ij} = 2\mu e_{ij} + \lambda \delta_{ij} \delta_{kl} e_{kl} - \gamma \delta_{ij} T - \alpha \delta_{ij} P \quad (5)$$

where ζ is equivalent liquid production
 α is Biot's parameter
 $M = 1/\phi\beta_p$
 $M_T = 1/\phi\beta_T$

Equation (4) describes the change in equivalent liquid strain due to rock strain, liquid pressure, and temperature represented by the three terms respectively on the right-hand side. Equation (5) gives the stress as dependent on the strain tensor, represented by the first two terms on the right-hand

side, and the temperature and pressure as described by the third and fourth terms respectively on the right-hand side.

Rock typically contains fractures that are cracks with two rough surfaces. These fractures may be filled partially or fully with clay or other materials. The constitutive models for rock fractures are summarized and reviewed by Ohnishi et al. (1996). For the current purpose of representing a physical behavior, we shall describe the THM behavior of a fracture with its normal in the 3 direction by the following equations, in close analogy to equations for solid rock:

$$\tau_i = C_{ij}U_j + \alpha\delta_{i3}P \quad i, j = 1, 3 \quad (6)$$

$$\zeta = \alpha \frac{U_3}{2b} + \frac{1}{M} P + \frac{1}{M_T} T \quad (7)$$

$$\frac{\partial \zeta}{\partial t} = \left[\frac{\rho_\ell k_\ell^f}{\rho_o n_\ell} (\nabla P + \rho_\ell g \nabla z) \right] \quad (8)$$

where C_{ij} is the deformation parameters for fractures (which could be stress or deformation-path dependent)

U_j is the relative displacement of the fracture surfaces in direction j

$2b$ is the fracture aperture

k_ℓ^f is the fracture permeability for liquid flow

Equations (6) and (7) are constitutive equations in terms of local values of normal and shear stresses and relative local deformation. The parameters α , M , and M_T are defined similarly to those of the rock matrix and are dependent on fracture roughness and fracture infill materials. Because of the difficulties of knowing the roughness and properties of infill materials, these quantities should probably be determined empirically.

Equation (8) describes fluid flow in the fracture plane. Equation (3) can be similarly applied for the flow of energy in the fracture. Because of the thinness of the fracture, no thermal gradient is assumed across the fracture aperture, and so heat is considered to flow only along the fracture plane.

The above equations, (1) – (8), can be extended to the case of unsaturated rocks. These equations were also developed by Noorishad and Tsang (1996). Other authors, instead of describing coupled processes in the rock matrix and fractures separately, have attempted to derive equivalent properties for a rock mass containing a large number of fractures. Thus the fracture rock is represented by an anisotropic elastic porous medium. One presentation of this approach and its validity in comparison with actual properties calculated using a discrete approach is given by Stietel et al. (1996).

Let us examine the eight equations again. The linkage of T, H and M occurs in two ways. Firstly, most of these equations link these three effects through terms in the equations. For example, Equation (1) has the pressure compressibility effect (second term on the left-hand side) and thermal expansion effect (third term on the left) interacting with the fluid flow represented by the right-hand side. In Equation (3), thermal capacity, strain energy, and convective flow energy, represented by

the three terms respectively on the left-hand side, combine to equate the thermal energy diffusion term on the right. Similarly one finds the same type of linkage in Equations (4) and (5). The second way linkage occurs between T, H and M is indirectly through the functional dependence of property coefficients. For example the density of fluid, ρ_ℓ , is temperature and pressure dependent and viscosity has a strong temperature dependence. Similarly the other coefficients may also have P, T, and τ dependence, though some to a much less degree than others.

The solution to these equations with coefficients dependent on P, T, and τ is in general a major challenge. From the theoretical standpoint, the three processes have widely different characteristic time constants and spatial scales. The thermal gradient has a relatively large time constant and spatial scale, since it is a function of the long heating cycle, and the thermal dispersivity smoothes out the effects of “local” spatial property variations. Mechanical effects, on the other hand, propagate through the rock with the speed of sound waves, and the deformation is strongly affected by faults and fractures, though much less so by medium property variations. Finally, the hydrologic flow and transport are very sensitive to smaller-scale medium heterogeneity, but with a time scale corresponding to the large solute transport times. Numerically these processes are commonly handled by different techniques, such as finite difference methods, finite element methods, discrete element methods, and others. To combine all of these into an efficient model for simulating coupled THM processes in fractured rock is no easy task.

A number of numerical codes have been developed to solve the coupled problem linking thermo-hydro-mechanical effects. The main ones are well summarized by Jing et al. (1995) and Stephansson et al. (1996). One of the codes, ROCMAS, has been developed by Noorishad et al. (1992) to solve the coupled Equations (1) – (8) based on a finite element model using mixed Newton–Raphson linearization within an incremental configuration. In the next section we shall use this code to study a coupled HM and a coupled THM problem, to provide physical insight into the results of linking these different effects.

TWO EXAMPLES OF COUPLED PROCESSES

The first example is on a coupled HM process in a constant injection test of a well that is intercepted by a fracture. Injection tests are often performed by bracketing the fracture between packers in the well to determine its permeability, which is usually quite low. In such cases, production tests would not be effective. If the injection pressure is high, e.g., above the lithostatic pressure, hydraulic fracturing will occur. However it has been shown that, even at pressures lower than that, the fracture aperture may be enlarged by the water pressure working against mechanical stress. This HM linkage was studied experimentally by Rutqvist (1995) and Rutqvist et al. (1998). In their experiment, a section of a well containing a fracture is isolated by packers. Then this well section is pressurized in a step-wise manner (Figure 1a). At each step, with pressure coming to a constant level, the flow into the well section also attains to a constant. The pressure is then increased to the next higher level. The results are plotted as pressure versus flow rates at the end of each pressure level (Figure 1b).

In this problem, a possible coupled HM effect occurs, namely that as the well section is pressurized, the fracture opens in response. This opening will increase the permeability of the fracture and thus less pressure rise is required to induce an increase in flow rate. This is illustrated

in Figure 1b, which shows two curves. The first is a straight line representing the linear relationship between pressure and flow rate to be expected for a non-deformable fracture, which is well known in conventional hydrology. The other is a curved line showing increasing steps of flow rate with decreasing steps of pressure, which corresponds to the effect that the fracture opens mechanically (increased aperture) at higher fluid pressures.

To test the above concept, an experiment was conducted (Rutqvist, 1995) in a 500-m deep-vertical borehole 56 mm in diameter, located in a crystalline rock at Lulea, Sweden. A fracture was identified at 417 m that was isolated by packers in the well. In the experiment, pressure was increased step-wise. The increased fluid pressure reduces the effective stress across the fracture, allowing the fracture aperture to increase. This is called the unloading path of the fracture in a hydraulic fracturing process in rock mechanics. At the end of this step-wise pressure increase, the experiment is continued by reversing the process and decreasing pressure step by step. This is the loading part of the fracture. The results are shown in Figure 2. During the unloading period, the pressure versus flow curve follows the pattern of a deformed fracture (curved line in Figure 1b). It is interesting to note that during the subsequent loading period, in which fluid injection pressure is reduced, flow decreases quickly until there is a backflow from the fracture to the well. This is an indication that the fluid is being "squeezed" back into the well under mechanical stress, which reduces the fracture aperture.

The second example of a coupled THM process is designed to replicate the effect of heating of a waste canister in a rock cavity on flow in nearby fractures. We use the ROCMAS code to study the thermohydromechanical environment surrounding a 5-kW heater in granite at a depth of 350 m. A horizontal fracture is assumed to lie 3 m below the heater midplane and to extend from the heater borehole to a hydrostatic boundary at a radial distance of 20 m from the borehole. The properties of rock and fracture are given in Table 1, and the two-dimensional axisymmetric (r,z) finite-element grid and some data are shown in Figure 3.

The heater drift, approximated by the cylindrical hatched area in Figure 3, is simulated by assigning a very low value of Young's modulus to the elements. Before the heater raises the temperature of a large volume of the rock, the flow of water from the hydrostatic outer boundary to the atmospheric ("zero" hydraulic pressure) borehole is high. Later, with the heated rock above the fracture expanding and the fracture aperture near the heater borehole closing, the flow decreases sharply, as shown in Figure 4.

The evolution of fracture aperture profile, together with the variations of the pressure and temperature distribution, is shown in Figure 5. As may be seen in the pressure-distance graph of this figure, at 0 day, before water in the fracture begins to flow, full hydrostatic pressure prevails in the fracture. This pressure diminishes rapidly at 0.25 day after the heater hole is opened to flow at atmospheric pressure and before major development of the thermal front. However, as thermal stresses are established, the fracture starts closing. As a result, the pressure inside the fracture starts rising, thus leading to the establishment of full pressure in the fracture after 14 days, similar to the 0 day case. These results may provide a better understanding of some of the observations made in the in-situ heater experiments in the Stripa granite (Witherspoon et al., 1981). The delayed responses of the extensimeters in these experiments may be explained by the closing of

Table 1. Materials properties used for the example application.

Material	Parameter	Value
Fluid	Mass density, ρ_s	997 kg m ⁻³
	Compressibility, β_p	5.13×10^{-10} GPa ⁻¹
	Dynamic viscosity at 20°C, η	10 ⁻³ N sm ⁻²
	Thermal expansion coefficient, β_T	3.17×10^{-4} °C ⁻¹
	Specific heat, C_{vw}	1.0 kcal kg ⁻¹ °C ⁻¹
Rock	Mass density, ρ_s	2.6×10^3 kg m ⁻³
	Porosity, ϕ	5.0×10^{-2}
	Permeability, k	10 ⁻¹⁷ m ²
	Young's modulus, E	51.3 GPa
	Poisson's ratio, ν	2.3×10^{-1}
	Biot's coefficient, α	1.0
	Biot's coefficient, M	5.0 GPa
	Thermal expansion coefficient, (linear) β	8.8×10^{-5} °C ⁻¹
	Specific heat, C_{vs}	2.1×10^{-1} kcal kg ⁻¹ °C ⁻¹
	Lumped thermal conductivity, K_M	3.18×10^{-3} KJ m ⁻¹ s ⁻¹ °C ⁻¹
Fracture	Porosity, ϕ	1.0
	Initial aperture, $2b$	10 ⁻⁴ m
	Initial normal stiffness, k_n	85 GPa/m
	Initial tangential stiffness, k_s	0.085 GPa/m
	Biot's coefficient, α	1.0
	Biot's coefficient, M	5.0 GPa
	Friction angle, ψ	30°
Cohesion, C	0.0	

the fracture. Similarly, aperture reduction leading to stoppage of water inflows into the heater boreholes (Nelson et al., 1981) also can be explained by the same phenomenon.

THREE CURRENT THM FIELD EXPERIMENTS

Concern over the consequences of coupled THM processes as they relate to nuclear waste repository performance has stimulated much experimental study. A number of laboratory and small-scale field experiments have been carried out on some of these processes. However, it is only recently that large-scale multiyear field experiments have been initiated to specifically study

coupled processes linking THM effects. Three major experiments that are ongoing or just completed are described in this section. They are summarized in Table 2.

As can be seen in Table 2, the Kamaishi experiment has just been concluded, but not all results have been published yet. The other two experiments are ongoing.

Table 2.

Experiment	Coupled THM Experiment	FEBEX Experiment	Drift Scale Heater Test
Location	Kamaishi, Japan	Grimsel, Switzerland	Yucca Mountain, USA
Site	Kamaishi Mines	Grimsel Underground Research Laboratory	Exploratory Studies Facility (ESF)
Expt. (heating-cooling) Period	1.5 years	5.5 years	8 years
Heating start date	October 1996	February 1997	December 1997
Heater length	2 m	2 heaters: ~ 10 m	9 drift heaters and 25 wing heaters: 45 × 20 m
Maximum temp. expected	100 °C	100 °C	200 °C
Remarks	Heater-bentonite system in vertical pit in fractured rock	Heater-bentonite blocks system horizontally in drift in fractured rock	Heater in drift with wing heaters in unsaturated volcanic tuff

Kamaishi Coupled THM Experiment

A THM experiment was conducted at the Kamaishi Mine in Japan from 1995 to 1998 by the Power Reactor and Nuclear Fuel Development Corporation (PNC). The purpose of the experiment was to study the mechanical effect of excavation on flow in fractured rock and the impact of a heater placed in an excavated pit with bentonite (clay) as a backfill material (PNC, 1997). The experiment was conducted at a depth of 250 m and simulated the condition of a waste canister storage pit in a potential nuclear waste repository in fractured hard rock (Figure 6). One objective of the test was to observe near-field coupled THM phenomena in situ and to build up confidence in coupled mathematical models of these processes. The experiment was divided into several phases, starting with a hydromechanical evaluation of the effects of excavation and ending with a fully coupled THM analysis of the heater test.

To conduct the experiment (Fujita et al., 1996), a test pit of 1.7 m in diameter and 5 m in depth was drilled in the floor of a 5 × 7 m alcove excavated off of an existing drift (Figure 6) at Kamaishi. The heat output from a waste package in the test pit was simulated by an electric heater, which was placed in the pit and surrounded by bentonite powder. Most of the measurements were

taken from locations within a radius of about 2 m from the center of the test pit, where most of the THM effects were expected to occur.

For the initial hydromechanical phase before emplacement of the heater and bentonite, measurements were focused on mechanical displacements of the test pit wall and along main fractures, and on the fluid pressure distribution and water inflow to the test pit. The fluid pressure distribution as a function of depth from the ground surface at Kamaishi does not correspond to the hydrostatic pressure gradient with depth due to continuous drainage in the existing drift system. At the horizon of the THM test the fluid pressure in the nearby 100-m area varies between 0.1 and 0.4 MPa, with an average pressure of about 0.3 MPa. Thus, the initial pore pressure at the site is much less than that expected at this depth.

The far-field properties and geometry affect the near-field behavior of fluid pressure and stress. In the rock mass at the level of the test drift, many fractures have NE strikes and steep dip angles. The minimum principal stress is subvertical, and the maximum principal stress is oriented almost perpendicular to the axis of the test drift. The maximum hydraulic conductivity is oriented parallel to the dominating fracture orientation and perpendicular to the maximum principal stress orientation. This indicates that the hydraulic conductivity is correlated to the fracture orientation rather than to the current in-situ stress.

Figure 7 presents the fractures mapped on the floor of the drift. These fractures have preferential NE strikes with steep dip angles (Figure 7a). There are too many fractures to include discretely in a finite element model. On the other hand, there may not be enough fractures to treat them as an equivalent continuum near the test pit. However, there are three large shear fractures or faults adjacent to the test pit, which strike approximately EW (Fractures 1, 2, and 3 in Figure 7b). These faults have been sheared and reported to be the most open fractures on the floor. They are up to 20 mm in thickness and containing some soft mineral filling. Similar fractures with the same strike and dip can be found on the roof, and these are also found to dominate the inflow into the drift.

During excavation of the test pit, the rock was strained to allow the stresses to be redistributed. Most of the strain was concentrated within a distance of three diameters from the test pit. As mentioned earlier, fluid pressure at the site was only 0.3 MPa and was not expected to cause any significant changes in fracture apertures. Thus, the hydromechanical coupling can be considered as a one-way coupling and is due to the disturbed stress field around the test pit. The disturbed stress field due to excavation first deformed the shape of the test pit cross section and second, changed apertures and hence permeabilities of nearby fractures. The former was obtained directly by measuring distances between four points on the wall of the test pit near the floor of the alcove, and the latter were estimated by borehole extensiometer measurements across the fractures that were intercepted by boreholes.

After the test pit was excavated, the rock near the pit surface was dehydrated because of ventilation; in other words, in the immediate neighborhood of the test pit, the rock is unsaturated and the local pore pressure can be negative. Nevertheless, water seeps into the test pit under hydraulic pressure. This seepage was measured by placing water-sorptive patches on the walls and measuring rates of water absorbed on these patches. The distribution of water rates around the pit wall is highly uneven, being largest along fracture traces on the wall. The total seepage rate into the test pit was

2 l/day. To increase the seepage rate, a shallow water pool was imposed on the alcove floor around the test pit. The rate was then found to be 280 l/day, and seepage distribution on the pit wall was again measured. These data, together with fracture distribution surveys on alcove floor and pit wall, were used to test computer models.

After the study of seepage into the test pit, a 2-m-long heater was emplaced and surrounded by bentonite. A one-year heating period was followed by a six-month cooling period, during which T, H, and M changes were carefully monitored all around the test pit. The unsaturated bentonite material experienced heating from the center of the test pit and wetting from the test pit wall. The heating caused water to vaporize and diffuse outwards, resulting in drying and possibly shrinkage near the center. The wetting from the rock saturated the bentonite and caused swelling and corresponding increase in pressure near the pit wall. These processes depend on parameters that are both temperature and saturation dependent. The coupled THM processes across the bentonite buffer are rather complex. In the rock, thermally induced coupled mechanical effects focused around fractures near the test pit on the alcove floor (Figure 7b) and at the bentonite–rock interface. The thermally induced coupled hydrologic effects included diffusive and convective flow in rock next to the test pit, and in the bentonite under variable saturation conditions. Although the experiment has now been concluded, the data have yet to be published. Some of the expected coupled processes in this experiment are summarized in Table 3.

Table 3. Some of the coupled THM processes expected in the Kamaishi experiment.

Linkage	Process Description
HM-1	Interaction between deformability and permeability of rock matrix and rock fractures during test pit excavation.
HM-2	Water flow under variable saturation conditions in bentonite–rock and bentonite–heater interfaces and also into bentonite, coupled with bentonite swelling.
TH	Heat transfer through rock matrix, fractures, bentonite, and their interfaces coupled with flow under both unsaturated and saturated conditions.
THM-1	Swelling pressure, multiphase flow with possible phase change (drying and wetting) in bentonite under a temperature gradient for variable-saturation conditions.
THM-2	Interaction between deformability and permeability of rock matrix, rock fractures, bentonite, and their interfaces during heating and cooling periods, involving both saturated and unsaturated flows.

The FEBEX Experiment

The Spanish nuclear waste management agency, ENRESA (Empresa Nacional de Residuos Radiactivos, S.A.), is conducting an in-situ experiment as part of their FEBEX program (ENRESA, 1996). The name FEBEX stands for Full-scale Engineering Barriers Experiment. The experiment (ENRESA, 1998) is located in a drift below the water table in the Grimsel

Underground Laboratory in Switzerland operated by NAGRA, the Swiss agency for nuclear waste management. The drift is 70.4 m long and 2.28 m in diameter. A number of radial boreholes were drilled from the drift into the Grimsel fractured rock. Then two heaters, each 4.54 m long and 0.9 m in diameter, were placed in the drift, separated from each other by 1 m. These heaters are along the axis of the drift, and are surrounded by packed bentonite blocks weighing 20–25 kg each. The radial boreholes are intensively instrumented to characterize the rock around the drift prior to heater and bentonite emplacement, as well as to monitor rock behavior during the heating and cooling phases. A total of 632 sensors of diverse types were installed in the bentonite blocks, the rock mass, the heaters, and the drift service zone to monitor temperature, humidity, total fluid pressure, mechanical displacement, and water pressure, etc. Figures 8 and 9 show a sketch of the experiment and the dimension of the test design, respectively.

The heaters were activated in February 1997, and will stay on for 5 yr, with an additional 6-month cooling period. During the 5-yr period, the temperature will reach and be maintained at 100°C near the heaters. At the end of the 5.5 years, the system will be dismantled to allow detailed sampling and observation for physical and chemical changes.

While the Kamaishi experiment focuses on a heater in a deposition pit in an alcove, the FEBEX experiment involves a drift, along which two heaters are emplaced. In the Kamaishi case, the buffer material was bentonite powder that was compacted in the test pit. In the FEBEX case, the buffer is in the form of bentonite blocks arranged around the horizontal heaters. The scale of the FEBEX experiment is significantly larger, the length of the two heaters together being 10 m, compared with the length of the single heater at Kamaishi, which was 2 m. Thus, the two experiments are good complements to each other, providing a range of data to understand coupled THM processes in heater-bentonite-fractured rock systems.

All the processes described in the previous section for the Kamaishi experiment are expected to occur in the FEBEX experiment. See Table 4. In addition, a number of other features are also important in the FEBEX case. They are included in Table 4, and are discussed below:

(a) Disturbed rock zone. During the excavation of the drift, the rock near the drift wall will be disturbed by stress redistribution and by excavation methods, especially near fault zones. Small fractures may be created and existing fractures may be deformed. Once the drift is constructed, dehydration will occur in rock near the drift wall, creating an unsaturated flow condition. After the drift is closed, the rock will be resaturated and water will flow into the drift under regional hydraulic pressure. The role of the disturbed rock zone on coupled HM processes during the whole stress redistribution-dehydration-saturation process is very interesting, and the FEBEX experiment will be used to study it.

(b) Disturbed zone–bentonite interaction. The emplacement of the unsaturated bentonite introduces a material with high suction near the rock. If the suction rate is high relative to the inflow rate from the rock, there is the possibility of further dehydration of the disturbed zone, reducing its effective permeability. At the same time, as the bentonite is wetted, a swelling pressure will be imposed on the disturbed zone.

Table 4. Some of the coupled THM processes expected in the FEBEX experiment.

Linkage	Process Description
HM-1	Interaction between deformability and permeability of rock matrix and rock fractures during test pit excavation.
HM-2	Water flow under variable saturation conditions in bentonite–rock and bentonite–heater interface and also into bentonite, coupled with bentonite swelling.
HM-3	Unsaturated water flow in gaps between bentonite blocks and bentonite swelling.
HM-4	Role of disturbed zone in rock near the drift wall on mechanical and hydraulic properties during dehydration and resaturation.
TH	Heat transfer through rock matrix, fractures, bentonite and their interfaces coupled with flow under both unsaturated and saturated conditions.
THM-1	Swelling pressure, multiphase flow with possible phase change (drying and wetting) in bentonite under a temperature gradient for variable-saturation conditions.
THM-2	Interaction between deformability and permeability of rock matrix, rock fractures, bentonite, and their interfaces during heating and cooling periods, involving both saturated and unsaturated flows.
THM-3	Interference between two heat sources on heating, water flow (wetting and drying), and swelling of bentonite blocks between the two heaters.
THM-4	Comparison of THM processes in fractured rock in the wet and dry parts of the drift.

Note: HM-1, HM-2, TH, THM-1 and THM-2 are identical to processes expected to occur in the Kamaishi experiment (Table 3), but the spatial and temporal scales are much larger in the FEBEX experiment.

(c) Gaps between bentonite blocks and between bentonite blocks and the rock or heaters. Flow of water in the gaps under a temperature gradient imposed by the heaters will cause bentonite swelling and sealing of these gaps. If the sealing rate is slow, the wetting and saturation of the blocks can occur from gaps between blocks. If the sealing rate is fast, there will be very uneven saturation of the bentonite system, with high saturation around block boundaries and low saturation in block centers. Because of this variable saturation spatially, there will be a complex distribution of swelling pressure and deformation in the system.

(d) Interference of the two heaters. The bentonite blocks between the two heaters will experience heating, vaporization, and drying from two sides as well as water wetting from the rock through interfaces.

(e) In the FEBEX drift, it was noticed that the part of the drift near one of the two heaters was much wetter than the other because of the presence of a fracture zone. First, this implies a possible uneven wetting of the bentonite blocks along the drift, unless the gap between the bentonite and the rock is so effective that water is quickly redistributed. Second, the comparative THM behavior of the fractured rock in the two parts of the drift under the temperature gradient may be significant and could unveil the characteristics of coupled THM processes at the site.

Extensive experimental data are being collected at FEBEX, and the results will be published in the coming years. A number of modeling efforts are already under way to make predictions and to perform evaluations of the experiment.

The Drift Scale Heater Test

To study technical issues related to the construction, operation, closure, and performance of a potential nuclear waste repository, the U.S. Department of Energy, Office of Civilian Radioactive Waste Management, is conducting a series of in-situ experiments in the Exploratory Studies Facility (ESF) at Yucca Mountain, Nevada. One of these experiments is the Drift Scale Heater Test (DST), whose purpose is to acquire an in-depth understanding of the coupled thermo-mechanical-hydrological-chemical processes anticipated in the rock mass around a repository (Dyer, 1997).

The experimental arrangement (Peters et al., 1997) is schematically shown in Figures 10 and 11. The drift to be heated is 47.5 m long and 5 m in diameter. Nine floor heaters are emplaced in the drift. In addition, 50 wing heaters have been placed in boreholes extending from the drift in a horizontal plane. Each of the floor heaters is 4.6 m long, and each of the wing heaters is 10 m long. The test is being conducted in unsaturated fractured tuff. The heaters were turned on in December 1997. Over a 4-yr heating period, the drift wall temperature will reach 200°C, and will be maintained at that temperature to ensure that coupled THM and chemical processes are properly observed. The heating period will be followed by a 4-yr cooling period. Approximately 3,500 measuring devices of various types have been installed in boreholes in the vicinity of the heated drift to monitor temperatures, rock displacements, rock moisture content, relative humidity, and pressures. Air permeabilities at various points will be measured at different stages of the experiment, and samples of water and gas will be collected periodically. Microseismic emissions, if any, will also be monitored.

Because the unsaturated volcanic tuff will be subject to temperatures as high as 200°C, significant evaporation and condensation is expected. Temporal changes in saturation will in turn strongly affect the effective permeability for fluid flow in the rock. Gravity also is an important factor in the downward flow of condensed water. Further, because the rock is highly fractured, such flow of condensed water will initially be in the fractures and will subsequently be imbibed into the rock matrix. Thus, the flow is highly complex and is dependent on the properties of the fracture-matrix interface, whose characteristics are still an open question. Mechanical strain in the neighborhood of the heater drift will be monitored, and water sampling will be carried out to obtain the chemical characteristics. The inter-linking of strain, temperature, and flow in this test will be investigated. Water chemistry will also give indications of THM system behavior.

Table 5 summarizes some of the coupled processes present in the Yucca Mountain Drift Scale Heater Test. Because of unsaturation, the system has a very strong TH linkage. A temperature change will affect the water saturation level of the rock, which will change the capillary suction and effective permeability to water flow (TH-1). Further, a process called the heat pipe effect is expected to occur, which is a very effective heat transfer mechanism (TH-2). In this process, water near the heater is evaporated and the vapor moves along fractures down the thermal gradient and condenses in the cooler region. The condensed water then moves in rock matrix under capillary suction toward the drier regions near the heat source. In general, vaporization (boiling) and condensation are expected to occur in and around the heater test region and boreholes with packers and other methods have been put in place to detect them and collect condensed water samples.

The Yucca Mountain ESF site is highly fractured, and fractures can open significantly due to stress redistribution in drift construction. Wang et al. (1997) measured permeabilities of packed intervals in boreholes approximately 0.6 m above an alcove in the ESF some distance away from the Drift Scale Heater Test area. The measurements were made before and after the excavation, and an increase in the geometric mean of permeabilities of one and half orders of magnitude was found. We expect this process to happen in the Drift Scale Heater Test area (HM).

Because of the high temperature (200°C) expected in the experiment, the THM linkage will include (a) fracture aperture changes, (b) convective and diffusive flow of gas-vapor and water under gravity, (c) boiling and condensation, and (d) matrix imbibition. All of these will interact and

Table 5. Some of the coupled THM processes expected in the Yucca Mountain Drift Scale Heater Test.

Linkage	Process Description
TH-1	Effective permeability in an unsaturated fracture-porous medium as a function of temperature gradient, saturation, and fracture matrix interaction.
TH-2	Heat pipe effect in an unsaturated fracture-porous medium, with vapor produced near heat source, diffusing in fractures down thermal gradient, condensed and flowing back in matrix under capillary suction.
HM	Opening of existing fractures during excavation and stress redistribution; flow in unsaturated fractures with modified apertures.
THM-1	Change in fracture apertures under the high temperature gradient, unsaturated flow in fractures under gravity, and matrix imbibition, with the phenomenon of boiling and condensation.
THM-2	Coupled THM processes in fractured porous medium under a high temperature gradient, with channelized flow because of fracture aperture variation and rock heterogeneity.

couple with each other in interesting ways (THM-1). Of particular interest in this THM linkage is the role of heterogeneity of the media—both heterogeneity in the fracture plane (i.e., variable apertures) and heterogeneity in the rock medium as a whole. It has been shown by Birkholzer and Tsang (1997) and Birkholzer et al. (1998) that flow in unsaturated fractures are highly channelized; i.e., they flow along preferred fast paths. The effect is dependent on the degree of heterogeneity, the level of water saturation, and fracture–matrix interaction. The coupled THM linkage upon this kind of channelized flow will be very interesting and will display behavior not normally expected for homogeneous media or constant-aperture fractures (THM-2).

Initial data and information are beginning to emerge from the Yucca Mountain Drift Scale Heater Test. A parallel modeling program is also under way to predict and to understand the system behavior over the next eight years.

SUMMARY AND CONCLUDING REMARKS

An overview of coupled processes linking THM effects in fractured rocks is presented in this paper. A formulation is given to show the linkage mathematically, which can be used as a basis for numerical solutions and for further developments. Two simple examples on HM and THM coupled processes are discussed to convey a physical insight into such couplings. Then, three current large-scale, long-term experiments are described. These tests are conducted specifically to explore and study coupled processes in situ.

After over 10 years of research, the study of coupled THM processes has reached an important stage, cumulating in large-scale in-situ experiments such as the three described in this paper. These experiments involve not only isolated coupled processes but a number of coupled processes occurring together. Because of the dimension of these experiments, the geologic structure of the experimental site may also be complex, presenting a particular challenge to data interpretation. Fortunately, the experimental design has allowed extensive monitoring with many sensors of diverse types. Hopefully, the data gathered in the monitoring program will help explain the behavior of the various coupled processes involved. We anticipate intensive activities and significant advances in the understanding of coupled processes in the next few years.

Acknowledgements

Reviews and comments by Lanru Jing of the Royal Institute of Technology, Stockholm, Sweden, and by John Apps and Jonny Rutqvist of Ernest Orlando Lawrence Berkeley National Laboratory, Berkeley, California, USA, are gratefully acknowledged. Collaboration and discussions with Jahan Noorishad, Jonny Rutqvist, Ove Stephansson, and participants of the International DECOVALEX project are very much appreciated. Thanks are also given to Julie McCullough for her careful technical editing. The paper is prepared with joint funding from the Swedish Nuclear Power Inspectorate (SKI), Stockholm, Sweden, and the Office of Energy Research, Office of Basic Energy Sciences, Engineering and Geosciences Division, of the U.S. Department of Energy, through Contract No. DE-AC03-76SF00098. This research used resources of the National Energy Research Scientific Computing Center, which is also supported by the Office of Energy Research of the U.S. Department of Energy.

Literature Cited

- Birkholzer J, Tsang CF. 1997. Solute channeling in unsaturated heterogeneous porous media. *Water Resources Research*, 33(10) 2221–2238
- Birkholzer J, Li G, Tsang CF, Tsang Y. 1998. Modeling studies and analysis of seepage into drifts at Yucca Mountain. Submitted to *Journal of Contaminant Hydrology*
- Dyer, JR. 1997. Progress in field testing and modeling activities at the Yucca Mountain site. *Proc. of FTAM Workshop*, December 15–16, 1997, Ernest Orlando Lawrence Berkeley National Laboratory, Berkeley, CA
- ENRESA. 1996. Test Plan for FEBEX Experiment, *Empresa Nacional de Residuos Radiactivos*, S.A., Spain
- ENRESA. 1998. Febex-Full-scale engineered barriers experiment in crystalline host rock: Pre-operational stage, Summary Report. Publicacion Tecnica Num 01/98. *Empresa Nacional de Residuos Radiactivos*, S.A., Madrid, Spain
- Fujita T, Sugita Y, Sato T, Ishikawa H, Mano T. 1996. Coupled thermo-hydro-mechanical experiment at Kamaishi mine. Plan. PNC Report, TN8020
- Haijink B, ed. 1995. *Testing and modelling of thermal, mechanical and hydrogeological properties of host rocks for deep geological disposal of radioactive waste*. Proc. of Brussels Workshop, European Commission Report EUR 16219, 298 pp.
- IJRMMS. 1995. Special Issue: Thermo-Hydro-Mechanical Coupling in Rock Mechanics (Guest ed. O Stephansson), *International Journal of Rock Mechanics and Mining Sciences*, 32(5) July
- Jing L, Tsang CF, Stephansson O. 1995. DECOVALEX – An international cooperative research project on mathematical models of coupled THM processes for safety analysis of radioactive waste repositories. In Special Issue on THM Coupling in Rock Mechanics in *Int. J. Rock Mech. & Min. Sci.*, 32(5) 387–98
- Nelson PH, Rachiele R, Remer JS. 1981. Water inflow into boreholes during the Stripa heater experiments. Report LBL-12574, Lawrence Berkeley Laboratory, Berkeley, California
- Noorishad J, Tsang CF. 1996. Coupled thermohydroelasticity phenomena in variably saturated fractured porous rocks—Formulation and numerical solution. In *Coupled Thermo-Hydro-Mechanical Processes of Fractured Media*, eds. O Stephansson, L Jing, CF Tsang, pp. 93–134. Elsevier Science Publishers. 575 pp.
- Noorishad J, Tsang CF, Witherspoon PA. 1992. Theoretical and field studies of coupled behavior of fractured rocks – 1. Development and verification of a numerical simulator. *Int. J. Rock Mech. Min. Sci. & Geomech. Abstr.* 29:401–9
- Ohnishi Y, Chan T, Jing L. 1996. Constitutive models for rock joints. In *Coupled Thermo-Hydro-Mechanical Processes of Fractured Media*, eds. O Stephansson, L Jing, CF Tsang, pp. 93–134. Elsevier Science Publishers. 575 pp.
- Peters M, Datta R, Wagner R, Boyle W, Yasck R. 1997. Progress in field testing and modeling activities at the Yucca Mountain site. *Proc. of FTAM Workshop*, December 15–16, 1997, Ernest Orlando Lawrence Berkeley National Laboratory, Berkeley, CA
- PNC. 1997. *DECOVALEX II Project, Definition for Test Case 2, Kamaishi*, DECOVALEX Secretariat, Royal Institute of Technology, Stockholm
- Rutqvist J. 1995. Determination of hydraulic normal stiffness of fractures in hard rock from hydraulic well testing. *Int. J. Rock Mech. Min. Sci. & Geomech. Abstr.* 32:513-23

- Rutqvist J, Noorishad J, Tsang CF, Stephansson O. 1998. Determination of fracture storativity in hard rocks using high pressure injection testing. *Water Resources Research*. In press
- Stephansson O, Jing L, Tsang CF. 1996. Coupled Thermo-Hydro-Mechanical Processes of Fractured Media, *Series on Developments in Geotechnical Engineering*, No. 79, Elsevier Science B.V., Amsterdam
- Stietel A, Millard A, Treille E, Vuillod E, Thoravel A, Ababou R. 1996. Continuum representation of coupled hydromechanic processes of fractured media: Homogenization and parameter identification. In *Coupled Thermo-Hydro-Mechanical Processes of Fractured Media*, eds. O Stephansson, L Jing, CF Tsang. Elsevier Science Publishers. 575 pp.
- Tsang CF. 1991. *Coupled Hydromechanical-Thermochemical Processes in Rock Fractures*, *Review of Geophysics*, 29(4) 537-51
- Tsang CF, ed. 1987. *Coupled Processes Associated with Nuclear Waste Repositories*. Academic Press Inc., San Diego
- Wang JSY, Trautz RC, Cook PC. 1997. Flow tests to quantify seepage into drifts. *Proc. of FTAM Workshop*, December 15–16, 1997, Ernest Orlando Lawrence Berkeley National Laboratory, Berkeley, CA
- Witherspoon PA, Cook NGW, Gale JE. 1981. Geologic Storage of radioactive waste, field studies in Sweden. *Science*, 211, 894–900

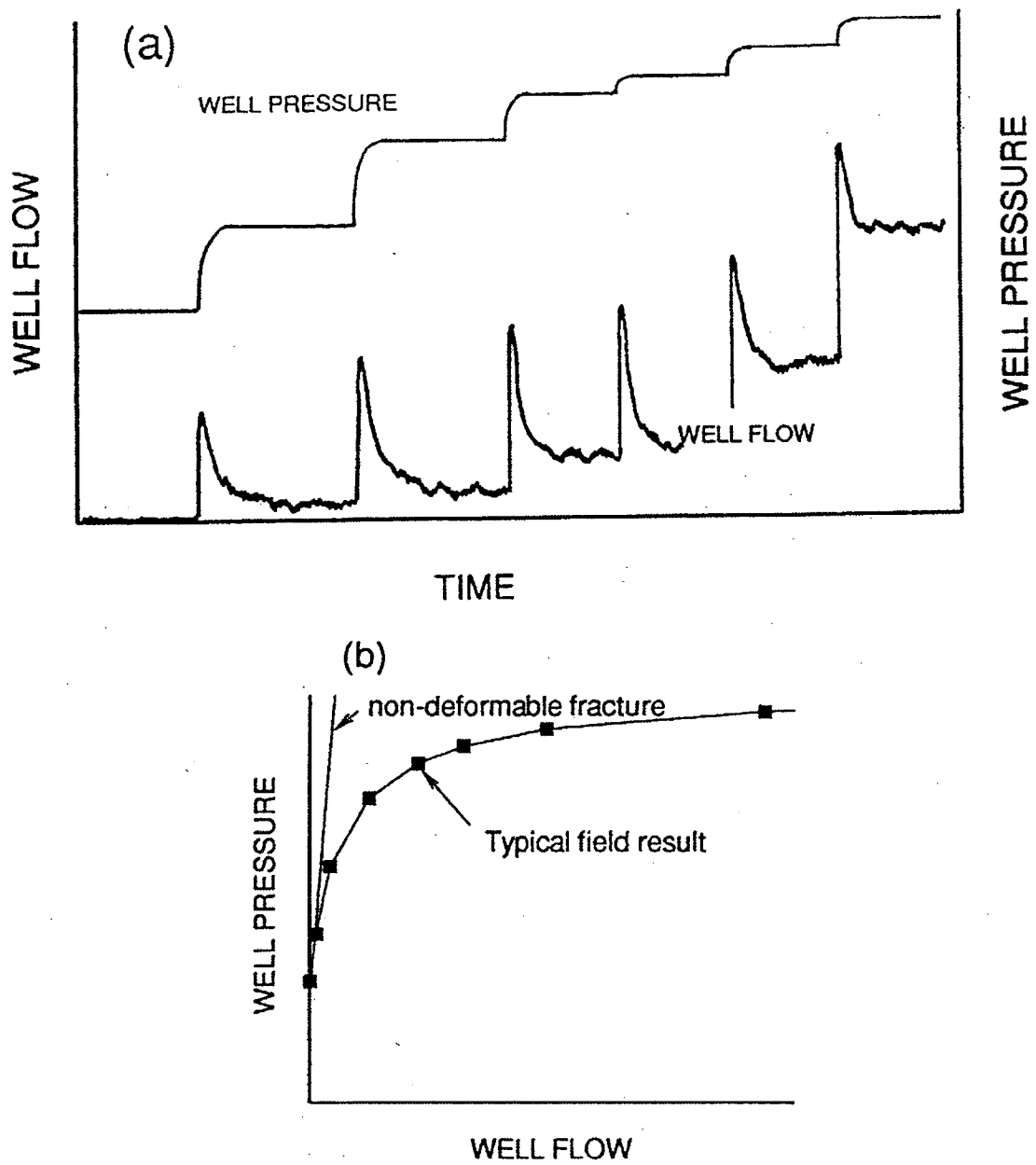


Figure 1. (a) A step-wise constant pressure injection test, with flow response; (b) a plot of pressure against flow at the end of each successive step (from Rutqvist, 1995).

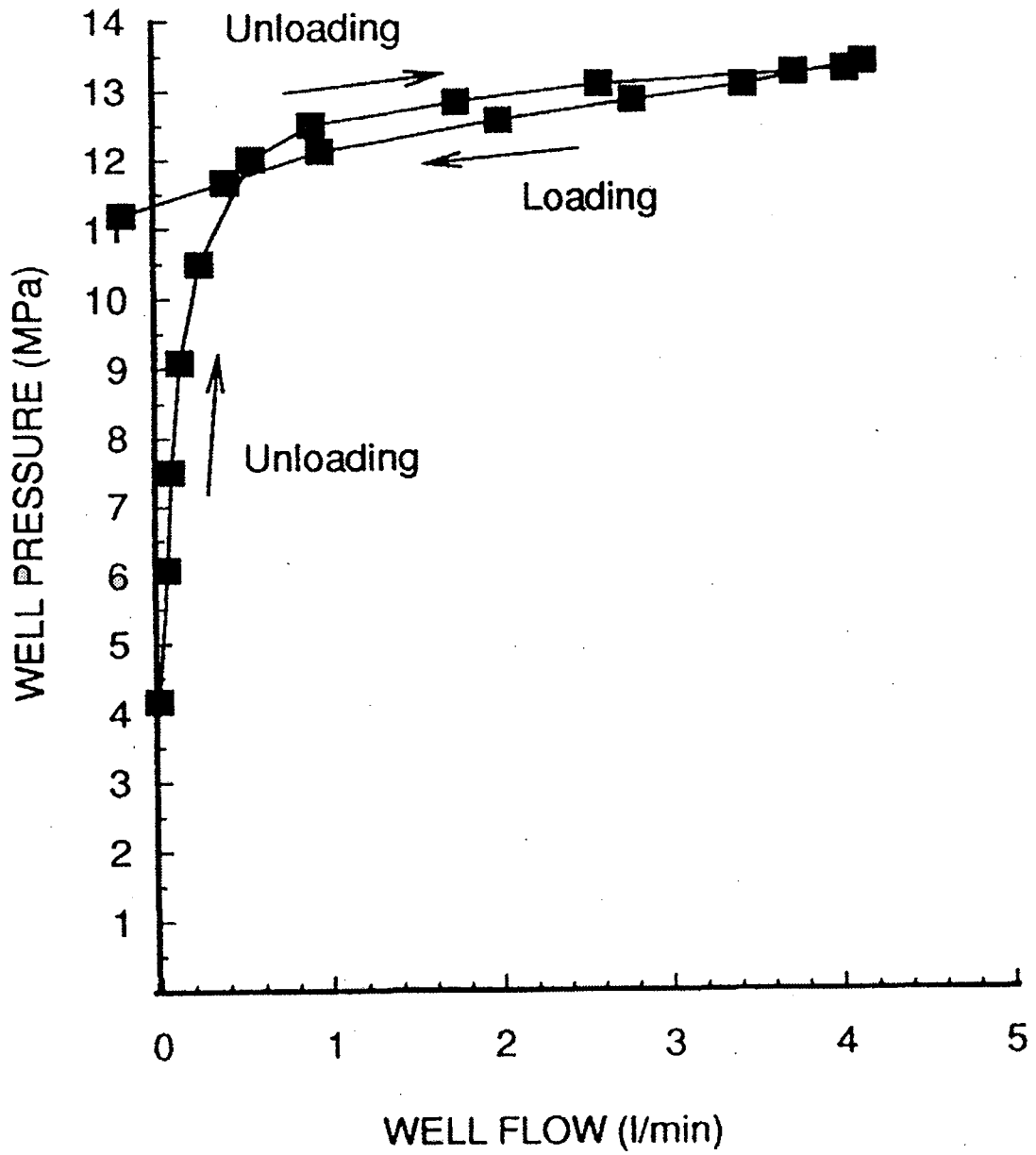


Figure 2. Field experimental results of pressure versus flow at the end of each step in a step-wise constant injection test. Unloading corresponds to increasing pressure when the effective stress is reduced. Loading corresponds to step-wise decrease of injection pressure (from Rutqvist, 1995).

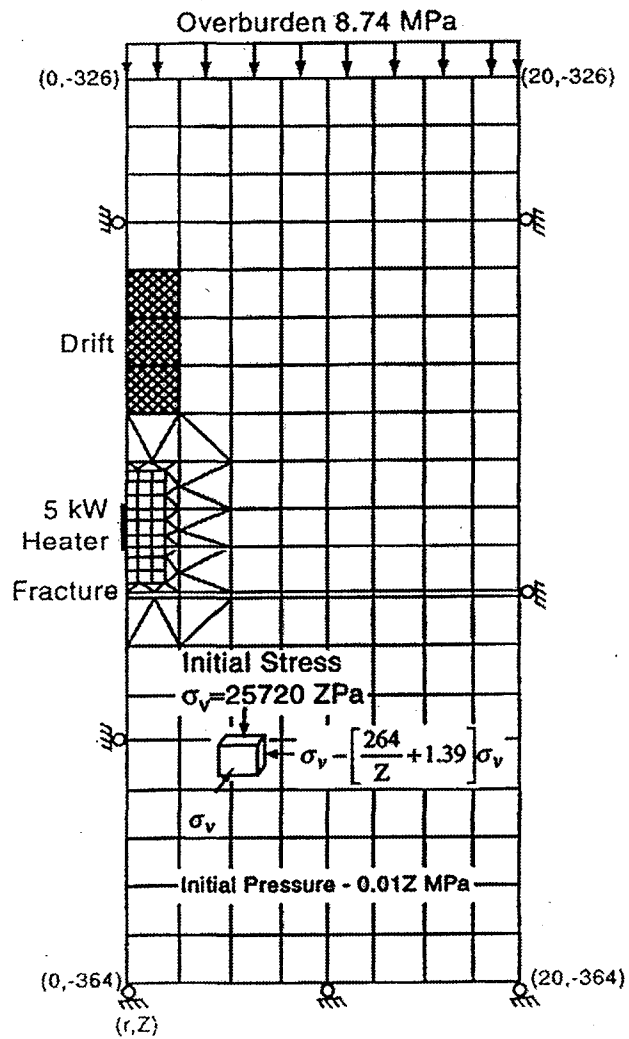


Figure 3. Vertical cross section of the finite element mesh around a heat source with a horizontal fracture just below the heater (from Noorishad and Tsang, 1996).

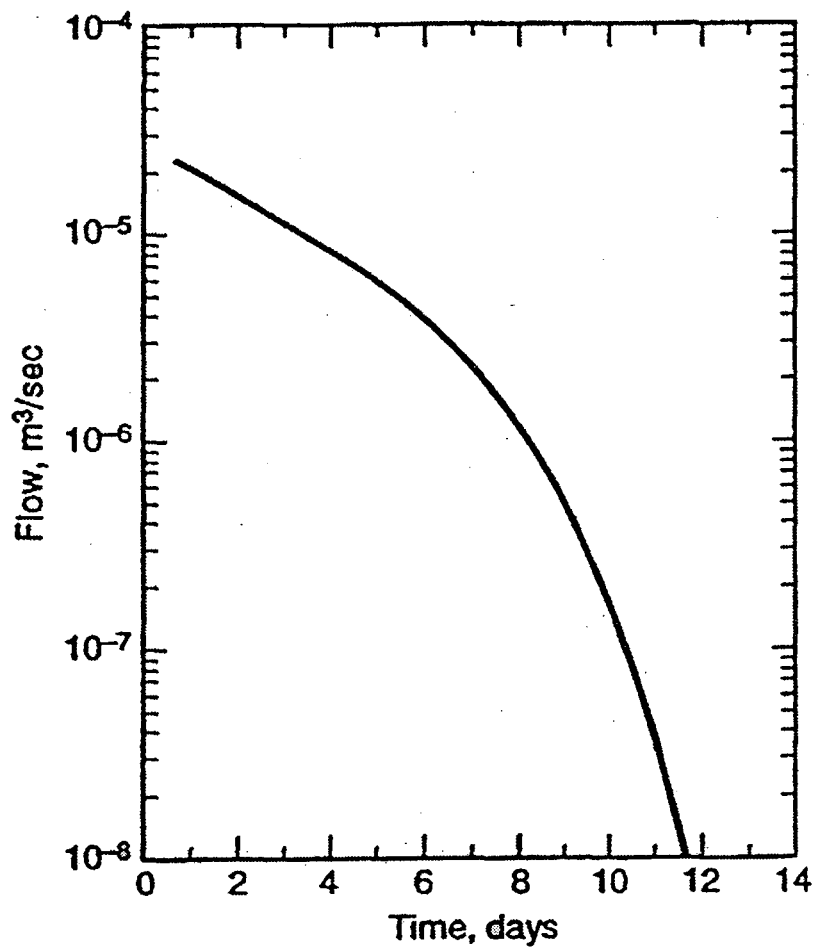


Figure 4. Variation of fluid inflow into the heater borehole as a function of time (from Noorishad and Tsang, 1996).

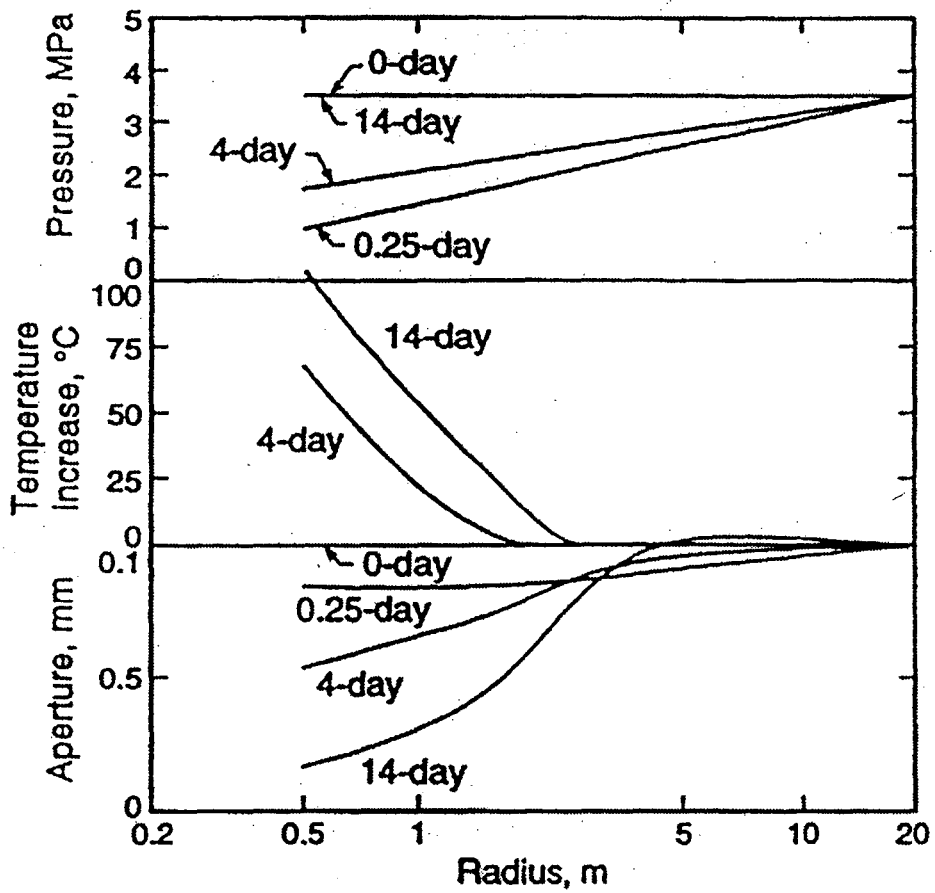


Figure 5. Pressure, aperture, and temperature profiles along the heater mid-plane for different times (from Noorishad and Tsang, 1996).

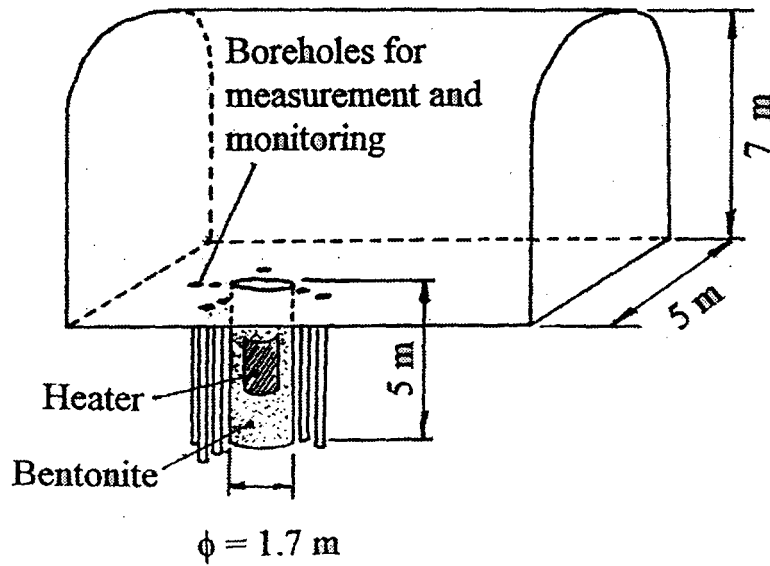
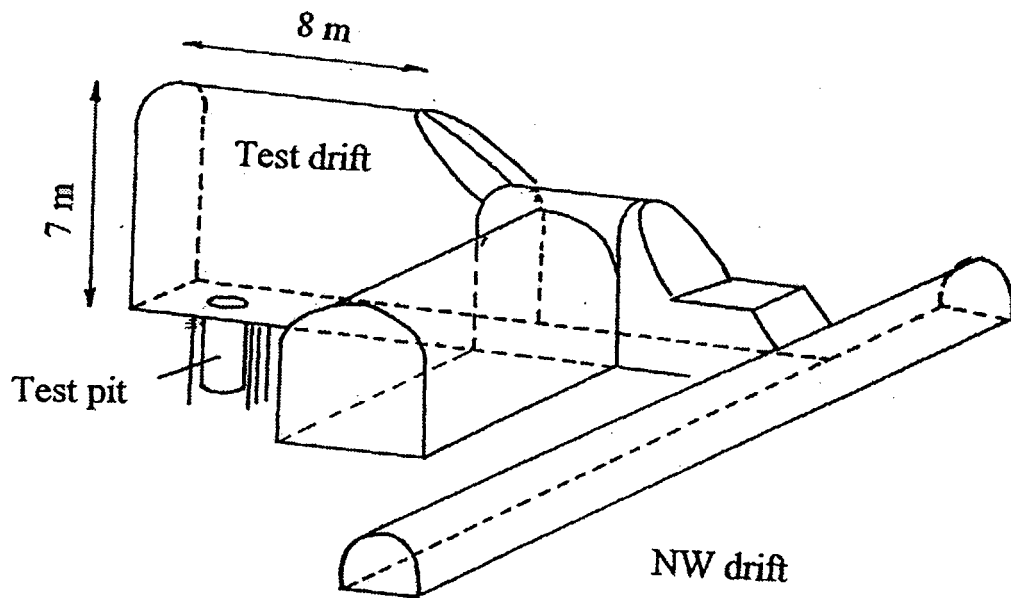
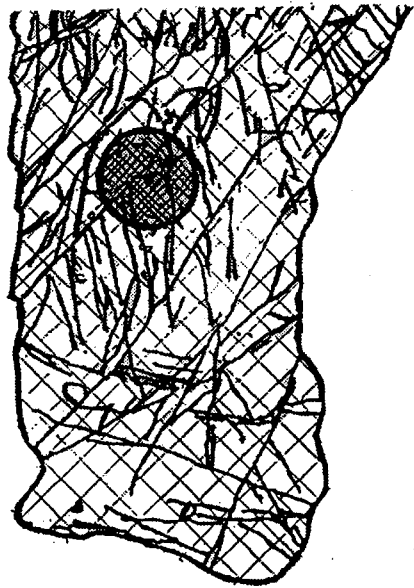
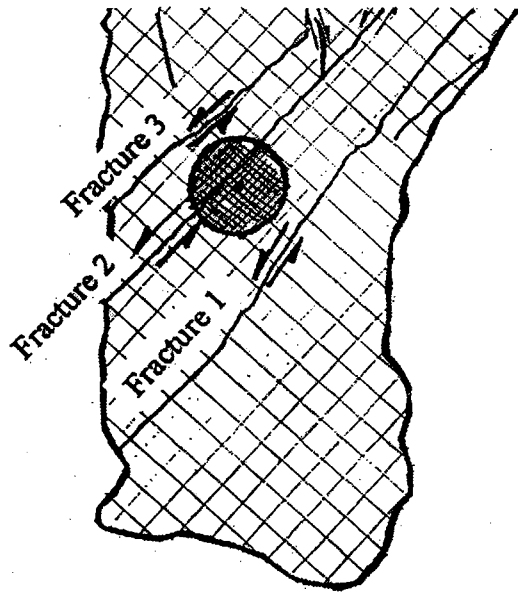


Figure 6. Arrangement of Kamaishi field experiment (from PNC, 1997).



(a)



(b)

Figure 7. Fracture map (left) on the floor of the drift where the test pit is drilled, and a simplified map (right) with only the major fractures (from PNC, 1997).

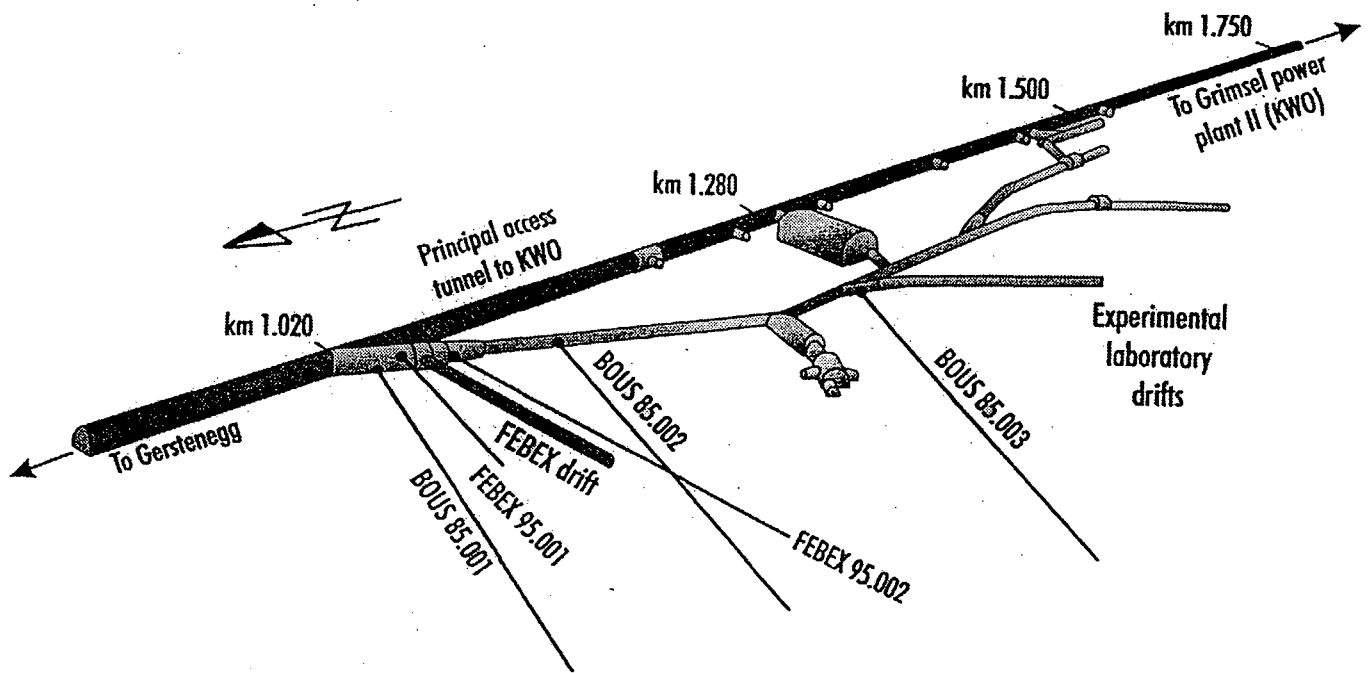


Figure 8. Location of the FEBEX experiment in the Underground Testing Facility in Grimsel, Switzerland. Scale is indicated in km along the main tunnel (from ENRESA, 1998).

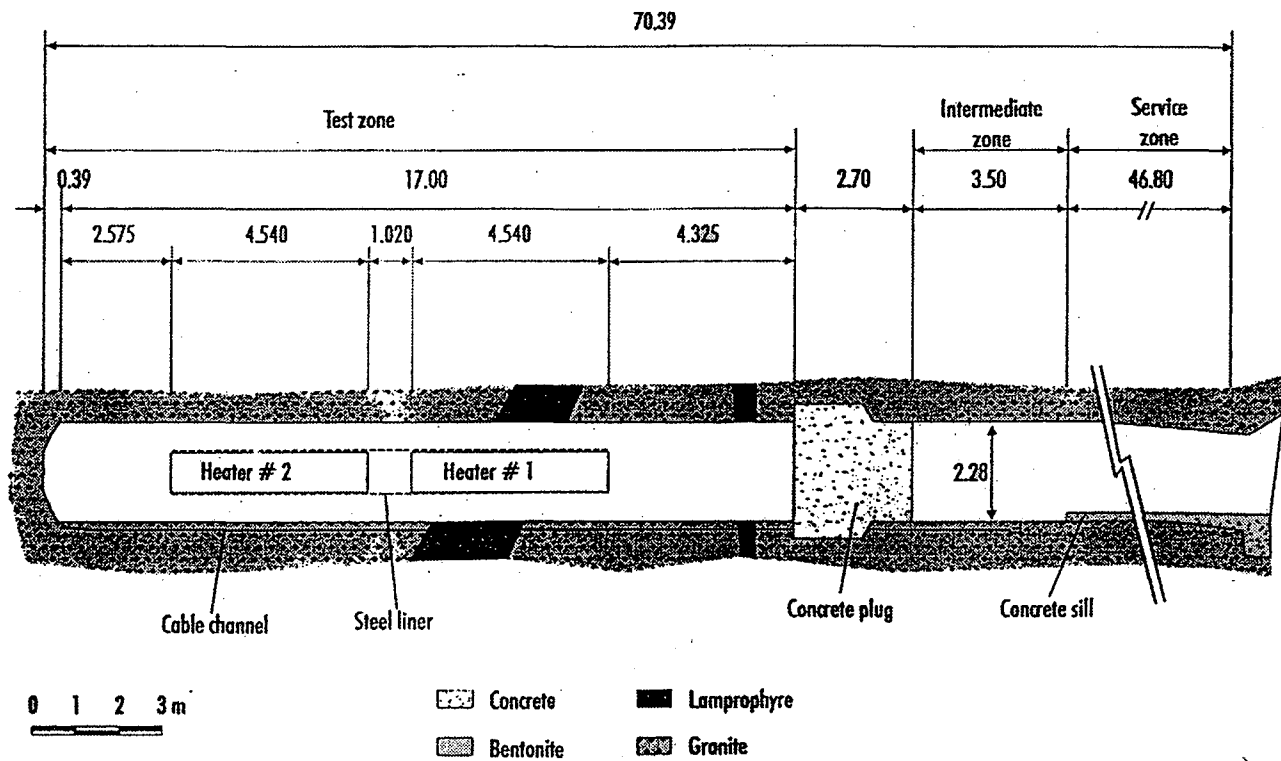


Figure 9. A closer view of the heater drift with 2 heaters; dimensions are in m (from ENRESA, 1998).

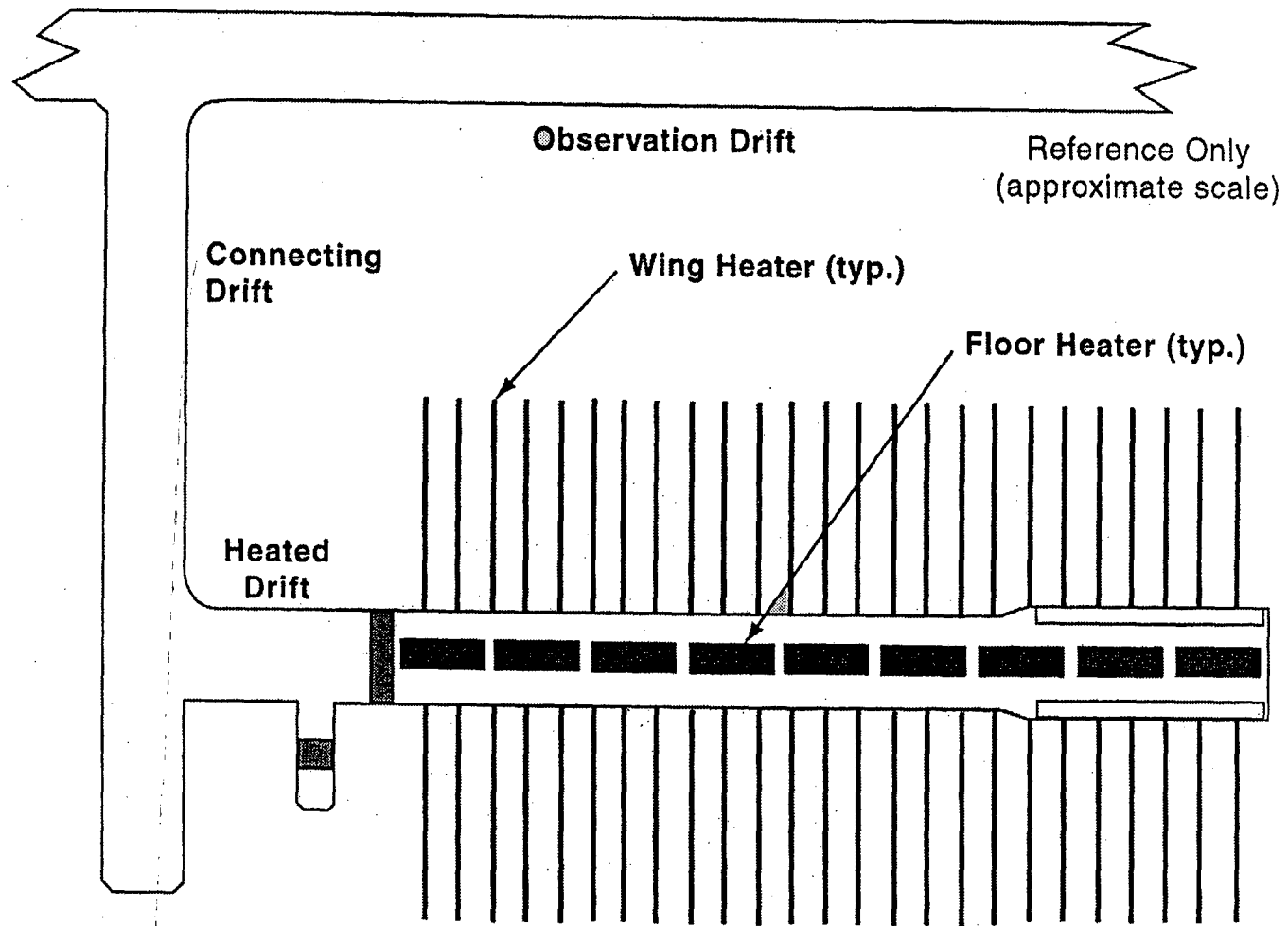


Figure 10. Arrangement of the Drift Scale Heater Test at the Exploratory Studies Facility at Yucca Mountain. Total length of drift heater is about 45 m and of each wing heater is 10 m (from Peters et al., 1997).

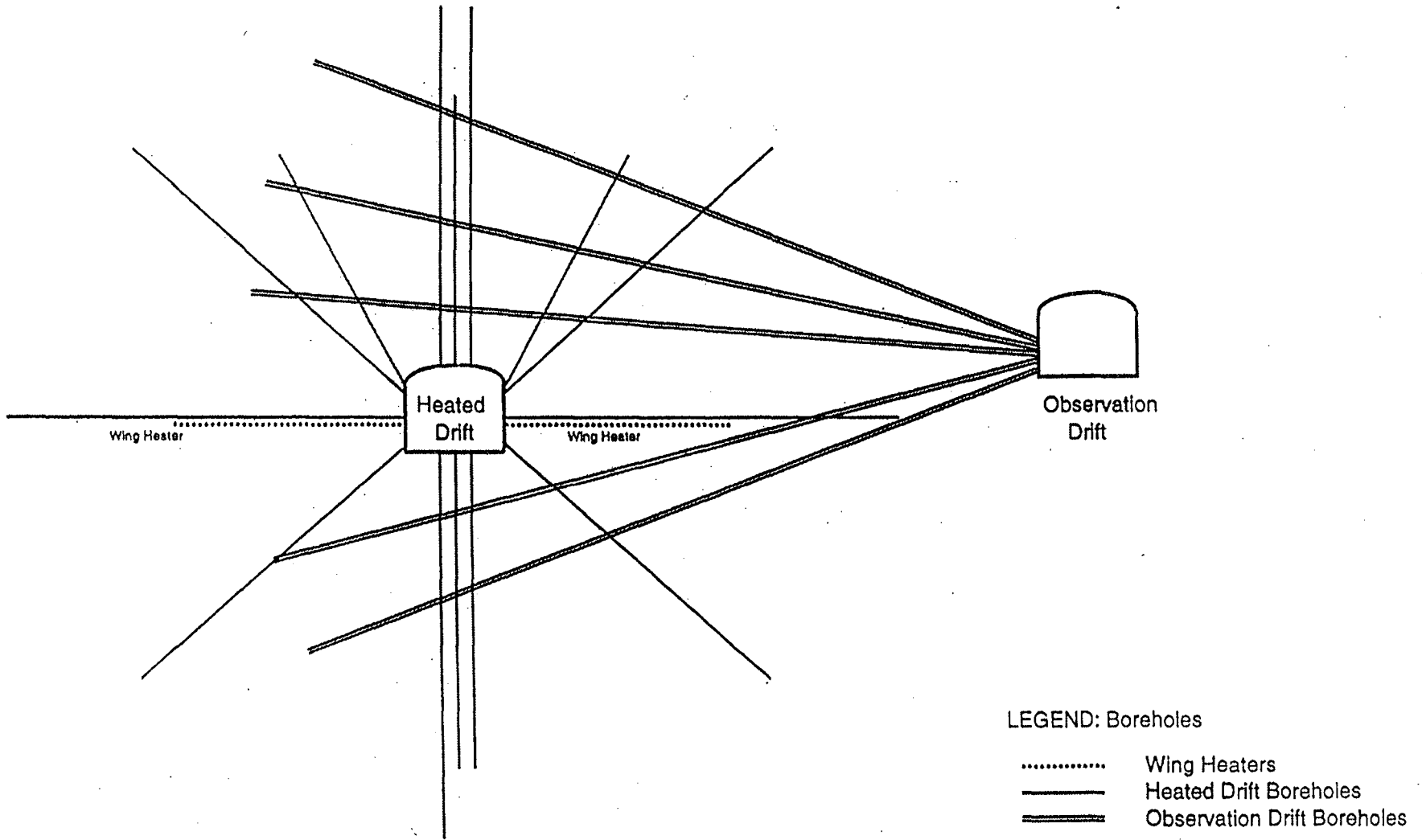


Figure 11. A cross section to illustrate the location of boreholes around the heater drift to monitor changes during the heater test. The diameter of the drifts is 5 m (from Peters et al., 1997).

**ERNEST ORLANDO LAWRENCE BERKELEY NATIONAL LABORATORY
ONE CYCLOTRON ROAD | BERKELEY, CALIFORNIA 94720**